Crystallization of brownian particles from walls induced by a uniform external force

Crystallization of Brownian Particles from Walls Induced by a Uniform External Force

Masahide SATO[1*], Hiroyasu KATSUNO[2†] and Yoshihisa SUZUKI[3]

[1] *Information Media Center, Kanazawa University, Kakuma-machi, Kanazawa, 920-1192, Japan*

[2] *Computer Centre, Gakushuin University, 1-5-1 Mejiro, Toshsima-ku, Tokyo 171-8588, Japan*

[3] *Institute of Technology and Science, The University of Tokushima, 2-1, Minamijosanjima, Tokushima, Tokushima, 770-8506, Japan*

Keeping the formation of colloidal crystal under a centrifugal force in mind, we study ordering of Brownian particles induced by a uniform external force. When the uniform external force is added, the particles move in the direction of the external force and the density of particles near walls becomes high. Ordering of particles starts on the walls, and successively ordering in bulk occurs near the walls. In bulk, both domains of the face-centered cubic structure and the hexagonal close-packed structure appear. By controlling the direction and the strength of the external force, the number of ordered particles and the distribution of cluster size are changed.

KEYWORDS: Colloidal crystal, Centrifugal force, Brownian dynamics

1. Introduction

Colloidal crystals are three-dimensional regular structures formed by colloidal particles with submicron size. The formation of colloidal crystals has received much attention for their application as photonic crystals. With regard to the distance between particles, the colloidal crystals are classified under two types. When the distance between particles is much longer than the diameter of particles, i.e the particles are packed loosely, the crystals are called non-close-packed colloidal crystals. They are created by using some techniques,[1–4] e.g. shear-annealing, controlling gradient of temperature, and controlling a PH gradient. Large non-close-packed colloidal crystals are made more easily and quickly than the close-packed col-

*E-mail: sato@cs.s.kanazawa-u.ac.jp

†Present address: Venture Business Laboratory, Nagoya University Furo-cho, Chikusa-ku, Nagoya 464-8603, Japan

loidal crystals in which the distance between particles is as long as the diameter of particles. The distance between particles in non-closed-packed colloidal crystals is tunable, so that the crystals have very attractive features as material for photonic crystals.[5,6] On the other hand, since closed-packed-colloidal crystals are able to be used as templates for inverse opals with perfect three-dimensional photonic bandgaps,[7] the close-packed colloidal crystals have received more attention than the non-closed-packed colloidal crystal.

So far, many groups have tried to create a large close-packed colloidal crystal without defects. Yin and co-workers[8] tried to form a large colloidal crystal without defects by using a template with a regular array of pyramidal pits. However, their colloidal crystal was so thin that it is necessary to increase the thickness of crystal. Davis and co-workers[9] took advantage of the sedimentation by gravitation and succeeded in creating a thick colloidal crystal. The use of gravitational force seems to be a good method to form large colloidal crystal, but there are some problems to solve in their experiment:[9] the crystal was narrowly columnar and the number of initial nucleation was hardly controlled. In order to enlarge the grain size, it is necessary to increase the area of the base of columnar grains and to decrease the number of nuclei formed in the initial stage. In simulations,[10,11] it is shown that large grains of hard sphere particles without defects are formed by changing the external force during sedimentation, but controlling the force during sedimentation is probably difficult in the experiment.[9]

In order to solve the problems in a previous study,[9] recently, Suzuki and co-workers[12,13] used a centrifugation method and succeeded in forming large three-dimensional colloidal crystals. They also pointed out the importance of the relation between the direction of centrifugal force and the grain size: the grain size of the colloidal crystal formed with a tilted force becomes larger than that with the centrifugal force perpendicular to a wall.

Our aim is to find conditions to form a large colloidal crystal by sedimentation, so that keeping the results of their experiments[12,13] in mind, we carry out Brownian dynamics simulations and study how crystallization of particles depends on the direction and the strength of a uniform external force. In § 2, we introduce the model. In § 3, we show the results of our simulation. We first show that ordering in bulk starts from the vicinity of walls with increasing the density of particles. Since ordering of particles on walls occurs faster than that in bulk, it is expected that structures formed on wall affect those in bulk. The external force probably affects ordering on walls. Thus, we investigate the effects of the inclination of an external force on ordering of particles on wall, and show how the structures on wall affect ordering of particles in bulk. Then, we observe structures in bulk and investigate the dependence of

ordering in bulk on the external force in detail. In § 4, we summarize our results and give brief discussions.

2. Model

The model we use is a very simple one.[14] We consider a three-dimensional system whose size is given by $L_x \times L_y \times L_z$. We use a periodic boundary condition in the y-direction, and consider walls in the x- and the z-directions. In the system, we put N sphere particles. When the mass of particles is m, the equation of the motion of the ith particle is given by

$$m\frac{\mathrm{d}^2\boldsymbol{r}_i}{\mathrm{d}t^2} = \boldsymbol{F}_i - \zeta\frac{\mathrm{d}\boldsymbol{r}_i}{\mathrm{d}t} + \boldsymbol{F}_i^{\mathrm{B}}, \tag{1}$$

where $\boldsymbol{r}_i$ is the position of the ith particle, $\boldsymbol{F}_i^{\mathrm{B}}$ is the random force, $\boldsymbol{F}_i$ is the sum of an external force and forces caused by an interaction between particles, and ζ is the frictional coefficient. $\boldsymbol{F}_i^{\mathrm{B}}$ satisfies the following relations: $\left\langle \boldsymbol{F}_i^{\mathrm{B}}(t)\right\rangle = \boldsymbol{0}$ and $\left\langle F_{ix}^{\mathrm{B}}(t)F_{ix}^{\mathrm{B}}(t')\right\rangle = \left\langle F_{iy}^{\mathrm{B}}(t)F_{iy}^{\mathrm{B}}(t')\right\rangle = \left\langle F_{iz}^{\mathrm{B}}(t)F_{iz}^{\mathrm{B}}(t')\right\rangle = 2\zeta k_{\mathrm{B}}T\delta(t-t')$, where T is temperature and k_{B} is the Boltzmann constant. The force $\boldsymbol{F}_i$ is expressed as

$$\boldsymbol{F}_i = F_{\mathrm{ext}}\mathbf{e}_{\mathrm{ext}} + \sum_{i\neq j}\boldsymbol{F}_{ij}, \tag{2}$$

where the first term is the external force by centrifugation and the second term is the force from other particles. F_{ext} is the strength of the external force, and $\mathbf{e}_{\mathrm{ext}}$ represents the unit vector parallel to the direction of the external force. The force caused by the interaction between the ith and jth particles is given by $\boldsymbol{F}_{ij} = -\nabla U(r_{ij})$, where we assume that the interaction potential $U(r_{ij})$ is a function of the distance $r_{ij} = |\boldsymbol{r}_{ij}| = |\boldsymbol{r}_i - \boldsymbol{r}_j|$ between them. For simplicity, we use the Weeks-Chandler-Anderson potential[15] as the interaction potential $U(r_{ij})$. Namely, $U(r_{ij})$ is expressed as

$$U(r_{ij}) = \begin{cases} 4\epsilon\left[\left(\dfrac{\sigma}{r_{ij}}\right)^{12} - \left(\dfrac{\sigma}{r_{ij}}\right)^{6} + \dfrac{1}{4}\right] & (r_{ij} \le r_{\mathrm{in}}), \\ 0 & (r_{ij} \ge r_{\mathrm{in}}), \end{cases} \tag{3}$$

where σ represents the diameter of particles and $r_{\mathrm{in}} = 2^{1/6}\sigma$.

We assume that the viscosity is so high that the acceleration rate, which is the term in the left side in eq. (1), is neglected. Thus, the velocity is approximately given by

$$\frac{\mathrm{d}\boldsymbol{r}_i}{\mathrm{d}t} = \frac{1}{\zeta}\left(\boldsymbol{F}_i + \boldsymbol{F}_i^{\mathrm{B}}\right). \tag{4}$$

In our simulation, we use σ , $\zeta\sigma^2/\epsilon$ and ϵ/σ as the units of length, time and force, respec-

tively. The normalized difference equation of eq. (4) is expressed as[16)]

$$\tilde{\boldsymbol{r}}_i(\tilde{t}+\Delta\tilde{t}) = \tilde{\boldsymbol{r}}_i(\tilde{t}) + \tilde{\boldsymbol{F}}_i\Delta\tilde{t} + \Delta\tilde{\boldsymbol{r}}_i^{\mathrm{B}}, \tag{5}$$

where $\tilde{\boldsymbol{r}}_i = \boldsymbol{r}_i/\sigma$ $\tilde{t} = t\epsilon/\zeta\sigma^2$ and $\tilde{\boldsymbol{F}}_i = \boldsymbol{F}_i\sigma/\epsilon$. We assume that perfectly elastic collision occurs between walls and particles. If $\tilde{x}_i(\tilde{t}+\Delta\tilde{t}) > \tilde{L}_x$ or $\tilde{x}_i(\tilde{t}+\Delta\tilde{t}) < 0$, the coordinate $\tilde{x}_i(\tilde{t}+\Delta\tilde{t})$ is replaced as $\tilde{L}_x - \tilde{x}_i(\tilde{t}+\Delta\tilde{t})$ or $-\tilde{x}_i(\tilde{t}+\Delta\tilde{t})$. The similar relation holds in the z-direction. The scaled displacement of the ith particle by the random force, $\Delta\tilde{\boldsymbol{r}}_i^{\mathrm{B}}$ satisfies $\left\langle\Delta\tilde{\boldsymbol{r}}_i^{\mathrm{B}}(t)\right\rangle = \boldsymbol{0}$ and $\left\langle\Delta x_i^{\mathrm{B}}(t)\Delta x_i^{\mathrm{B}}(t')\right\rangle = \left\langle\Delta y_i^{\mathrm{B}}(t)\Delta y_i^{\mathrm{B}}(t')\right\rangle = \left\langle\Delta z_i^{\mathrm{B}}(t)\Delta z_i^{\mathrm{B}}(t')\right\rangle = 2\tilde{R}^{\mathrm{B}}\Delta\tilde{t}\delta(t-t')$, where $\tilde{R}^{\mathrm{B}} = k_{\mathrm{B}}T/\epsilon$.

In our model, we neglect hydrodynamic effects. During sedimentation by centrifugal force, the hydrodynamic effects[17–20)] may not be neglected. However, since the centrifugal force in the experiment[13)] is much weaker than that in other experiments,[21–25)] the hydrodynamic effects may be smaller than those in other experiments. Thus, in order to simplify the model, we neglect the hydrodynamic effects and carry out simulation.

3. Results of simulation

First, we carry out a simulation with 8788 particles. The system size is given by $L_x = L_y = L_z \approx 24.8$, so that the volume fraction is 0.3. Initially, we set particles at random. We move the particles without an external force for a sufficiently long time. Then, we add the external force, set time t to 0, and carry out the simulation. Thus, the effects of the initial positions of particles is neglected. The parameters are $\tilde{F}_{\mathrm{ext}} = 0.5$, $\tilde{R}^{\mathrm{B}} = 0.1$ and $\Delta\tilde{t} = 4.0\times10^{-4}$. The drift velocity by the external force and the diffusion coefficient are expressed as F_{ext}/ζ and $k_{\mathrm{B}}T/\zeta$, respectively. Thus, the Peclet number P_{e} is given by $P_{\mathrm{e}} = F_{\mathrm{ext}}\sigma/k_{\mathrm{B}}T = \tilde{F}_{\mathrm{ext}}/\tilde{R}^{\mathrm{B}} = 5$.

Figure 1 shows snapshots in a late stage of sedimentation. The directions of the forces are $(0,0,1)$ in Fig. 1(a) and $(1,0,1)/\sqrt{2}$ in Fig. 1(b), so that the particles gather in the upper side and in the upper left, respectively. Since there are walls at $z = L_z$ and $x = L_x$, the particles are arranged regularly on the planes.

In Fig. 1, we cannot see the structure in bulk well, so that we change the view point and observe the time evolution of the structure in bulk. Figure 2 shows snapshots with the force $0.5(0,0,1)$ with a view from the y-direction. We show the positions of particles with dots. In an early stage (Fig. 2(a)), the particles are not sufficiently gathered in the upper side, but a few thin layers of particles, which is parallel to the top wall, are already formed. The particles attached to side walls also seem to start forming a few layers parallel to the walls. In Fig. 2(b), we clearly find the layers of particles parallel to the side wall grow from the upper region. In Fig. 2(c), most of the particles have gathered in the upper region. The layers parallel to the

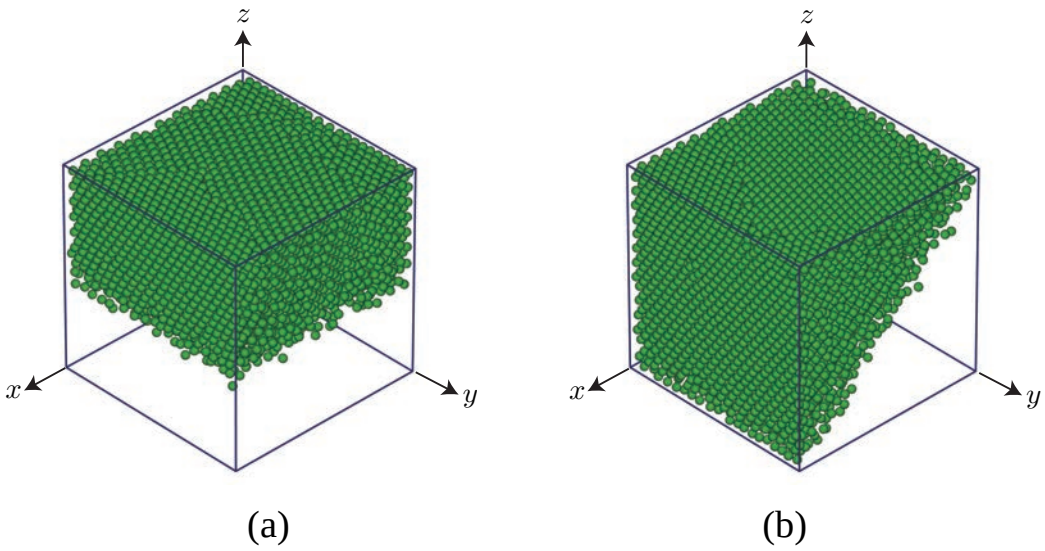

Fig. 1. (Color online) Snapshots of the positions of particles in the last stage in a simulation. The strength of force is $F_{\rm ext} = 0.5$, and the directions of the external force are (a) $(0, 0, 1)$ and (b) $(1, 0, 1)/\sqrt{2}$. Time is $\tilde{t} = 1000.0$.

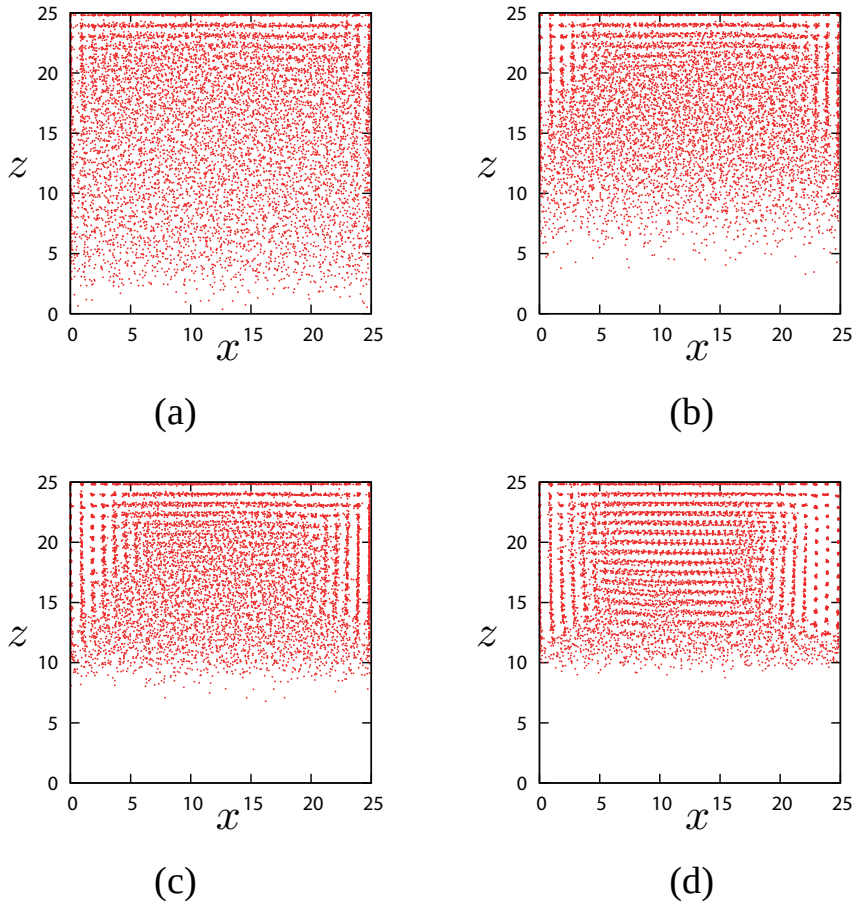

Fig. 2. (Color online) Snapshots with a view from the y-direction. Red dots show the positions of particles projected in the $x - z$ plane. The direction of the external force is $(0, 0, 1)$ and its strength is $F_{\rm ext} = 0.5$. Time is (a) $\tilde{t} = 10.0$, (b) $\tilde{t} = 20.0$, (c) $\tilde{t} = 30.0$, and (d) $\tilde{t} = 500.0$.

side walls are wider than those parallel to the top wall in the upper region. Disordered region is still left in the center of the system. In a later stage (Fig. 2(d)), particles in the center region are ordered and form layers parallel to the top wall. The width of the layers parallel to the side walls is thiner than that parallel to the top wall.

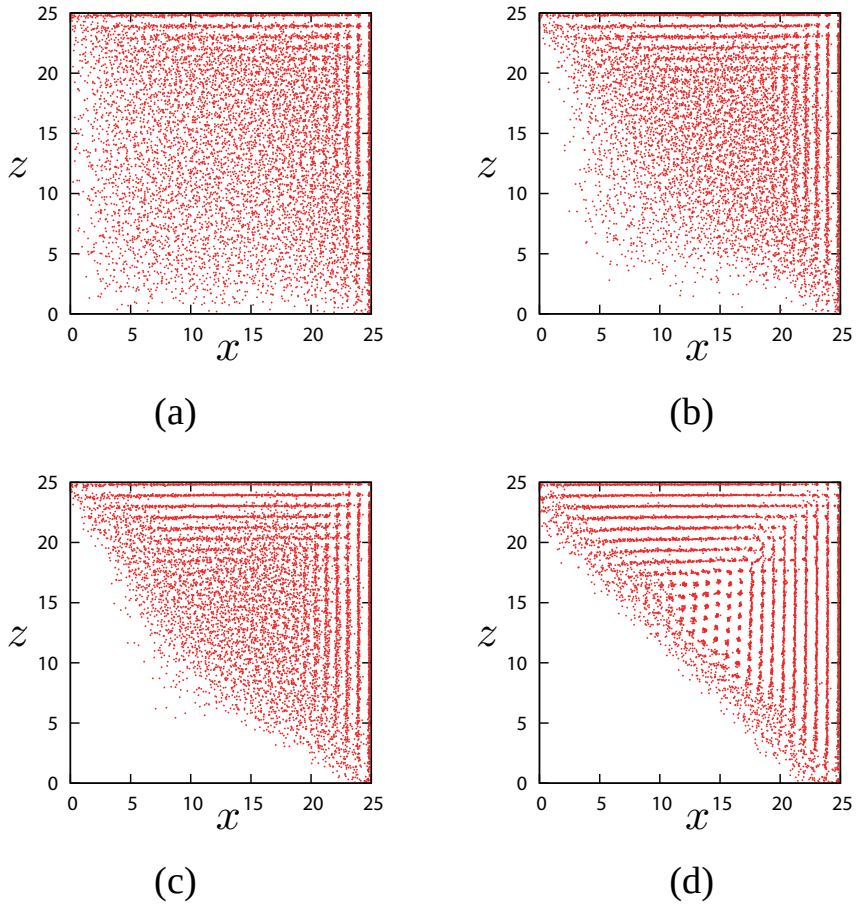

Fig. 3. (Color online) Snapshots with a view from the y-direction. Red dots show the positions of particles projected in the $x-z$ plane. The direction of the external force is $(1,0,1)/\sqrt{2}$ and its strength is $F_{\rm ext} = 0.5$. Time is (a) $\tilde{t} = 10.0$, (b) $\tilde{t} = 20.0$, (c) $\tilde{t} = 30.0$, and (d) $\tilde{t} = 500.0$.

Figure 3 shows snapshots during crystallization with the tilted force $0.5(1,0,1)/\sqrt{2}$. Since the x-component of the external force is equal to the z-component, the top wall is equivalent to a side wall $x = L_x$. In an early stage (Fig. 3(a)), thin layers parallel to the top and the right side wall start forming. In Figs. 3(b) and (c), particles near the two walls are already ordered, but particles in the center region are still disordered. In a later stage (Fig. 3(d)), the particles in the center region have been ordered. The positions of particles form spot-like pattern in the center region and linear pattern near the walls.

From Figs. 2 and 3, ordering of particles on walls first occurs and then ordering in bulk

gradually occurs from the walls, so that ordering on walls probably affects ordering in bulk. Thus, we estimate ordering of particles attached on the walls. Since the particles are pressed against walls by an external force, the particles should form a triangle lattice in order to increase density on particles. To see ordering of particles on walls in detail, we introduce a order parameter ψ_k which shows the sixfold orientation order around the kth particles. The definition of ψ_k is given by

$$\psi_k = \frac{1}{n_k} \left| \sum_{m=1}^{n_k} \mathrm{e}^{6\mathrm{i}\theta_{km}} \right|, \tag{6}$$

where n_k is the number of neighboring particles of the k particles. In our simulation, we assume that the particles behave as hard particles without size. When the particles form a close-packed structure in bulk and a close-packed plane appears parallel to a wall, the distance from the wall to center of particles on the second layer of the close-packed plane is $\sqrt{2}r_{\mathrm{in}}/2$. Thus, with taking account of thermal fluctuations, we consider that particle attaches on the wall if the distance between a particle and a wall is smaller than $0.5r_{\mathrm{in}}$. If both the kth particle and the mth particle attach on the wall at $z = L_z$ and the distance between the two particles in the plane $\sqrt{(x_k - x_m)^2 + (y_k - y_m)^2}$ is smaller than r_{c}, we treat the mth particle as a neighboring particle.[26–28] The repulsion between the particles acts when $r_{km} < r_{\mathrm{in}}$, so that with taking account of the displacement by thermal fluctuations, we use $1.1r_{\mathrm{in}}$ as r_{c} in our analysis. In eq. (6), θ_{km} is the angle between the vector $(x_k - x_m, y_k - y_m)$ and the positive x-direction. In our simulation, we regard the particles with $\psi_k > 0.9$ as ordered particles and color them. If the ordered particles line parallel to the x-axis, we color them in red (dark gray). With increasing the angle of the line of particles from the side, we gradually change the color. The color becomes yellow (light gray) when the angle is 30°. Owing to the sixfold orientation order, the color returns to red when the angle is 60°. We color them white when $\psi_k < 0.9$, and green (dark) particles are the particles which do not attach to the top wall. Figure 4 shows snapshots of particles attached on the top wall. When the force is in the z-direction (Fig. 4(a)), on the top wall a triangle lattice is formed near edges at $x = L_x$ and $x = 0$. Square lattices are formed in the center region. On the other hand, with a tilted force (Fig. 4(b)), although there are separated into two domains, almost all the top wall is covered with triangle lattices. Thus, ordering on wall with a tilted force is better than that with a force normal to the wall.

Next, we investigate how ordering in a wall affects ordering in bulk. To estimate the order in bulk in detail, we introduce orientation order parameters $Q_l(i)$ and $w_l(i)$,[29–31] which

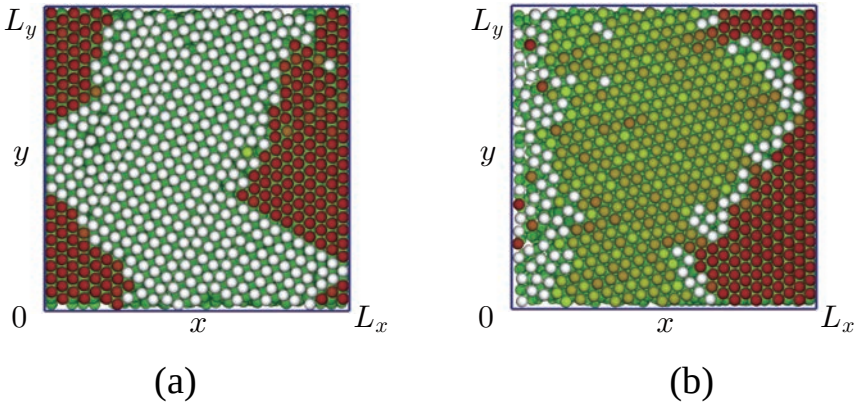

Fig. 4. (Color online) Snapshots of particles attached on the top wall, which are viewed from z-direction. The strength of the external force is $F_{\rm ext} = 0.5$, and its direction is (a) $(0, 0, 1)$, and (b) $(1, 0, 1)/\sqrt{2}$. Red and yellow particles are the particles form a triangle structure, and white particles are others.

represent the local orientation order around the ith particle. $Q_l(i)$ is defined as

$$Q_l(i) = \sqrt{\frac{4\pi}{(2l+1)} \sum_{m=-l}^{l} |q_{l,m}(i)|^2}, \tag{7}$$

where

$$q_{l,m}(i) = \frac{1}{n_{\rm n}} \sum_{j=1}^{n_{\rm n}} Y_l^m(\theta_{ij}, \phi_{ij}). \tag{8}$$

The angles θ_{ij} and ϕ_{ij} represent the polar angle and the azimuthal angle of $\boldsymbol{r}_{ij}$, respectively. $Y_l^m(\theta_{ij}, \phi_{ij})$ is the spherical harmonics and $n_{\rm n}$ is the number of neighboring particles. If a close-packed structure is formed, the distance between particles is $r_{\rm in}$. However, by taking account of thermal fluctuations, we regard the jth particle as one of the neighbors of the ith particle if $|\boldsymbol{r}_{ij}|$ is smaller than $1.1r_{\rm in}$. The parameter $w_l(i)$ is defined as

$$w_l(i) = \frac{1}{g_l^{3/2}} \sum_{m_1+m_2+m_3=0} \begin{pmatrix} l & l & l \\ m_1 & m_2 & m_3 \end{pmatrix} q_{l,m_1}(i) q_{l,m_2}(i) q_{l,m_3}(i), \tag{9}$$

where g_l is defined as

$$g_l = \sum_{m=-l}^{l} |q_{l,m}(i)|^2. \tag{10}$$

In eq.(9), the integers m_1, m_2 and m_3 run from $-l$ to l with satisfying the condition $m_1 + m_2 + m_3 = 0$, and the term in the parentheses is the Wigner 3-j symbol.[32)]

By the external force, the density of particles in bulk becomes as high as possible, so that the expected structure in bulk is the hcp structure or the fcc structure. Thus, in order to distinguish the two structure, we calculate Q_6, Q_4 and w_4. Figure 5 shows the distributions

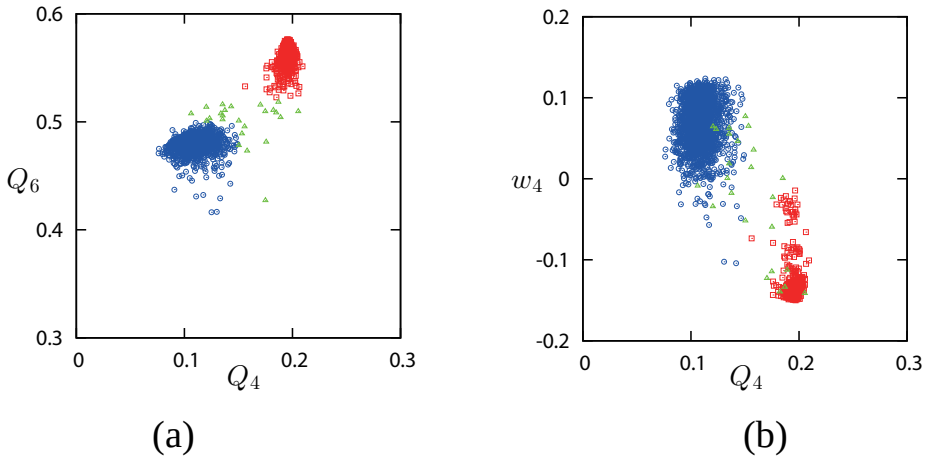

Fig. 5. (Color online) Distribution of the hcp structure and the fcc structure in (a) the Q_6-Q_4 plane and (b) the w_4-Q_4 plane, Red open squares, blue open circles, and green open triangles represent the particles with hcp structure, fcc structure and disordered structure, respectively. The data is the same as we used in Fig. 2(d).

of the structures on parameter planes. There are two spots in the Q_6-Q_4 plane. When we calculate Q_6 and Q_4, we neglect the particles which do not have 12 neighboring particles, so that the points which correspond to particles with the body-centered-cubic (bcc) structure do not appear on the parameter planes. Hereafter, we regard the structure of particles with $Q_6 > 0.52$ and $Q_4 > 0.15$ as the fcc structure and that with $Q_6 < 0.5$ and $Q_4 < 0.15$ as the hcp structure.[33] In Q_4-w_4 plane, it is expected that a spot for the fcc structure appears at the lower right and that for the hcp structure appears at the upper left.[31,34] Under the criterion we used, the spots in the Q_4-w_4 appears at the expected positions.[31,34]

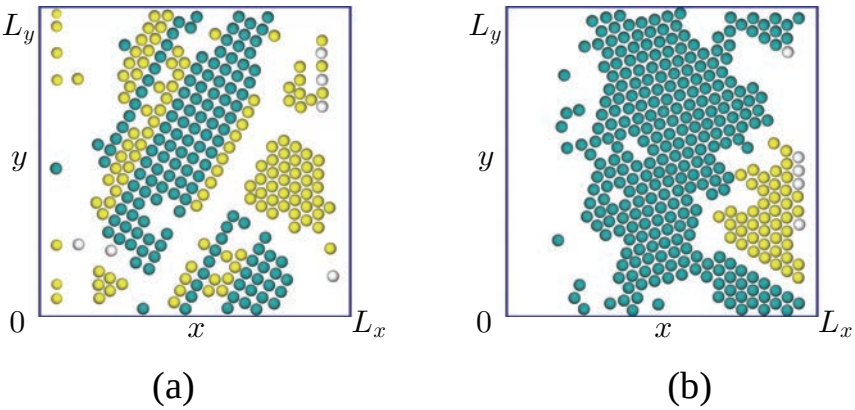

Fig. 6. (Color online) Snapshots of particles in the first layer in bulk, which are viewed from z-direction. The strength of the external force is $F_{\text{ext}} = 0.5$, and its direction is (a) $(0, 0, 1)$, and (b) $(1, 0, 1)/\sqrt{2}$. Blue and yellow particles are the particles with the fcc structure and the hcp structure, and white particles are others.

To investigate how ordering of particles on wall affects ordering in bulk, we pick out the particles in the first layer in bulk, which is directly under the particles on the top wall, and compare ordering of them with ordering on the top wall (Fig. 4). Fig. 6 shows the positions of ordered particles in the first layer in bulk, where we drew the particles with 12 nearest neighbors. Blue particles, yellow particles and white particles are the particles with the local fcc structure, the particles with the local hcp structure, and the disordered particles, respectively. Fig. 6(a) shows the positions of ordered particles under the particles shown Fig. 4(a). Square lattice of particles, which is a $\{1, 1, 0\}$ surface of the fcc structure, is formed under the square lattice on the layer attached on the top wall. With the tilted force (Fig. 4(b)), the triangle lattices are formed around an edge at $x = L_x$ and in the center. In the first layer in bulk (Fig. 6(b)), a $\{1, 1, 1\}$ face of the fcc structure and $\{0, 0, 0, 1\}$ face of the hcp structure are formed. Thus, we find that the structure in bulk depends on that in the top wall.

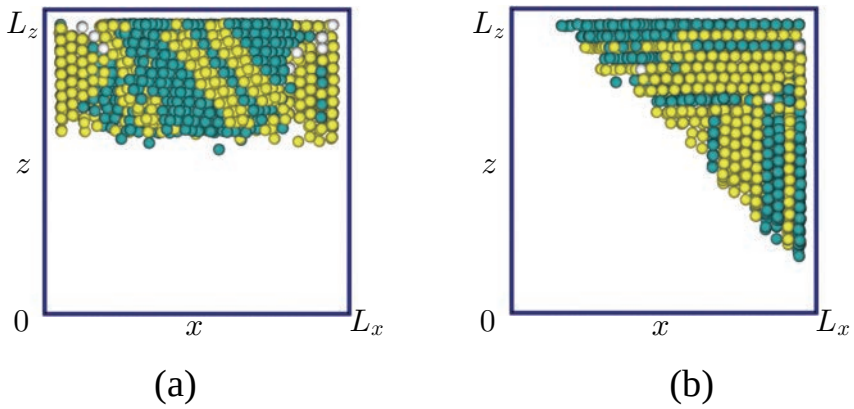

Fig. 7. (Color online) Snapshots with a view from $-y$-direction at $\tilde{t} = 500.0$, where the particles with 12 nearest neighbors are drawn. The strength of the external force is $F_{\text{ext}} = 0.5$, and its direction is (a) $(0, 0, 1)$ and (b) $(1, 0, 1)/\sqrt{2}$. Blue particles and yellow particles represent the particles with the local fcc structure and the local hcp structure, respectively. White particles show the particles with other structure or in disorder.

Figure 7 shows all the ordered particles in bulk. When the direction of the force is $(0, 0, 1)$ (Fig. 7(a)), the local hcp structure is much more than the local fcc structure near the side walls. In the region, the c-axis of the hcp structure is normal to the walls, and one of the $\{1, 0, \overline{1}, 0\}$ face is parallel to the plane $y = 0$. Far from the side walls, the local fcc structure is more than the local hcp structure. In the region, epitaxial growth from the top wall occurs. When the direction of the force is $(1, 0, 1)/\sqrt{2}$ (Fig. 7(b)), particles with fcc structure appear near the walls, and the $[1, 1, 1]$ direction of the local fcc structure is perpendicular to the walls. In the center region, the local hcp structure is mainly formed.

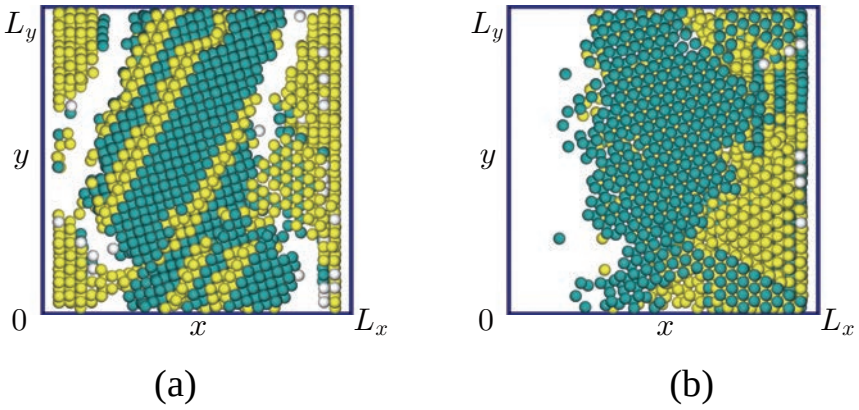

Fig. 8. (Color online) Snapshots with a view from z-direction at $\tilde{t} = 500.0$, where the particles with 12 nearest neighbors are drawn. The strength of the external force is $F_{\text{ext}} = 0.5$, and its direction is (a) $(0, 0, 1)$ and (b) $(1, 0, 1)/\sqrt{2}$. The meanings of colors are the same as those in Fig. 7.

We change the view point and see the same system again. Figure 8 shows the snapshots, which are seen from the z-direction. When the direction of the force is $(0, 0, 1)$(Fig. 8(a)), we can find that there is space between the hcp structure growing from the side walls and the fcc structure in the middle region, which grows from the top wall. The space represents the disordered region and is caused by encounter with crystals formed on the different walls. When the direction of the force is $(1, 0, 1)/\sqrt{2}$ (Fig. 8(b)), a large islands with the local fcc structure appear in the center region. The island forms triangle structure, so that $\{1, 1, 1\}$ face of the fcc structure is formed.

In the above, we have studied how ordering on wall affects on ordering in bulk. Then, we study the dependence of ordering of particles on the direction and strength of the external force. Hereafter, we carry out simulation with a larger system: system size is $L_x = L_y = L_z = 41.3$ and the number of particles is 13500, so that the volume fraction is 0.1. Figure 9 shows the dependence of $\langle\bar{\psi}_{\text{s}}\rangle$ on the tilting angle with some strength of external forces. θ represents the angle between the z-direction and the direction of force. $\bar{\psi}_s$ is the average of ψ_i over the whole of a wall in the last stage, and $\langle\bar{\psi}_s\rangle$ shows the average over some individual runs. In our analysis, the number of runs is 40. Ordering of particles occurs on three walls $z = L_z$, $x = L_x$ and $x = 0$ with $\theta = 0^\circ$ and 90°. Since the volume fraction is small, particles only attach on the walls $z = L_z$ and $x = L_x$ with the other angles, and the particles attaching on the wall $x = 0$ are neglected. When the external force is normal to a wall ($\theta = 0^\circ$), a lot of particles simultaneously attach on the top wall. There is not sufficiently extra space in the plane, so that particles cannot move in the plane easily. With increasing the strength of the external force, the particles, which also prevent for particles on walls from moving,

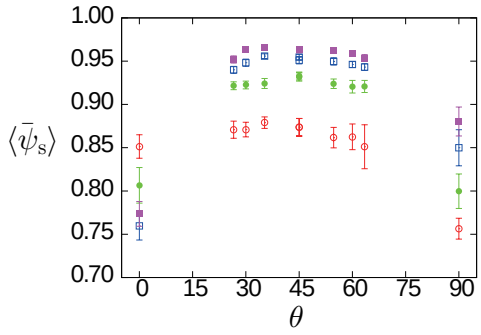

Fig. 9. (Color online) Dependence of the saturated value of $\langle\bar{\psi}\rangle$ on the angle. Open circles, solid circles, open squares, and solid squares show dependence of the saturated value of $\langle\bar{\psi}\rangle$ with the strength of the force 0.5, 1.0, 2.0 and 4.0, respectively.

come behind more quickly, Thus, $\langle\bar{\psi}_s\rangle$ decreases with increasing the strength of the external force. With a tilted force, the density of particles on walls increases from an edge and there is sufficiently extra spaces in another side. The particles can move easily and particles can form a triangle space from an edge, so that $\langle\bar{\psi}_s\rangle$ is larger than that with $\theta = 0°$. However, the external force normal to the wall decreases with increasing the tilting angle. The component of the external force, which presses the particles to the wall, is 0 when $\theta = 90°$, so that $\langle\bar{\psi}_s\rangle$ with $\theta = 90°$ becomes again small.

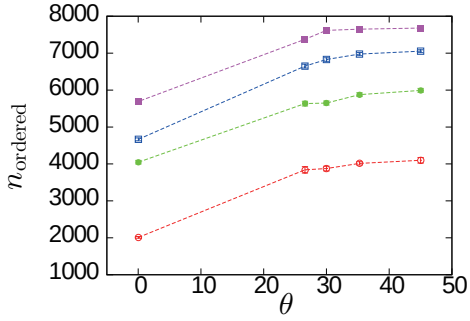

Fig. 10. (Color online) Dependence of the number n_{ordered} of ordered particles in bulk on the tilting angle and the strength of force. Open circles, solid circles, open squares, and solid squares show the dependence with the strength of the force 0.5, 1.0, 2.0 and 4.0, respectively.

Figure 10 shows the dependence of the number of ordered particles in bulk on the tilting angle and the strength of the external force. The number of ordered particles, which is the sum of the numbers of the particles with the local hcp structure and the local fcc structure, increases with increasing the strength of the external force. As shown in Fig. 2, solidification occurs from walls. When the domains grown from distinct walls meet, disordered particles

are left in the region. Solidification occurs from two walls with a tilted force. On the other hand, solidification occurs from three walls with $\theta = 0°$. Thus, when the direction of the external force is normal to a wall, disordered particles are left more than that in solidification with the tilted force. In Fig. 8(a), we can confirm that there is two large regions where there are hardly ordered particles. Thus, the number of ordered particles with $\theta = 0°$ is less than that with the tilting angle.

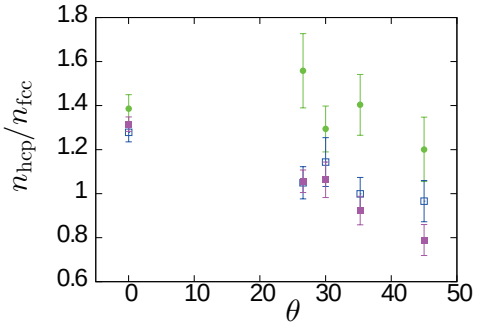

Fig. 11. (Color online) Dependence of the ratio of the number $n_{\rm hcp}$ of particles with the local hcp structure to that $n_{\rm fcc}$ of particles with the local fcc structure on the tilting angle and the strength of force. Solid circles, open squares, solid squares show the strength of the force 1.0, 2.0 and 4.0, respectively.

The ratio of the number $n_{\rm hcp}$ of particles with the local hcp structure to that $n_{\rm fcc}$ with the local fcc structure also depends on an external force. Figure 11 shows the dependence of $n_{\rm hcp}/n_{\rm fcc}$ on the external force. In each angle, $n_{\rm hcp}/n_{\rm fcc}$ decreases with increasing with the strength of force. When the strength of the force is 1.0, the maximum of the ratio seems to appear at about 25°. With other strength of force, the ratio decreases with increasing the angle.

From practical point of view, it is important to form a large domain of colloidal crystal. Thus, we also investigate how the cluster size changes with a external force. Figure 12 shows how the force affects the relation between the domain number and domain size. When the direction of the force is $(0, 0, 1)$ (Fig. 12(a) and (b)), the number of large domains with the local hcp structure increases with increasing the strength of the external force, but the change in form of distributions of the domain size is small: the domain number gradually decreases with increasing the domain size. Figure 12(c) shows the distribution of cluster size with tilted force $4(1, 0, 1)/\sqrt{2}$. Comparing Fig. 12(b) with Fig. 12(c), we find that the change of the form of the distribution causes by tilting the angle of the external force. When the direction of the force is tilted, although there is left a peak of the number of domains whose is smaller

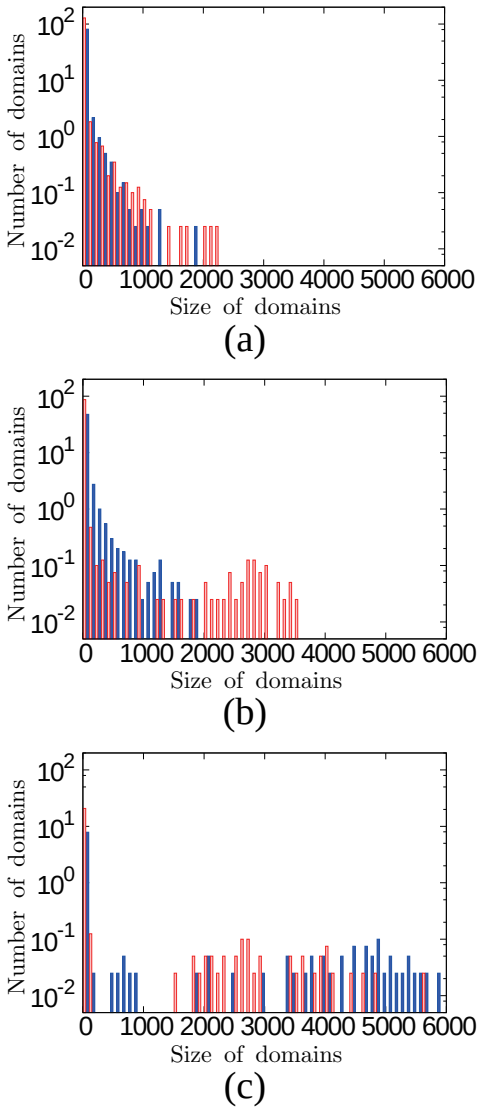

Fig. 12. (Color online) Relation between the number of domains and the domain size with (a) the force $(0, 0, 1)$, (b) $4(0, 0, 1)$, and (c) $4(1, 0, 1)/\sqrt{2}$. Red (light) and blue (dark) columns represent the numbers of the domains of the local hcp structure and the local fcc structure, respectively. The data are averaged over 40 runs.

than 100, the numbers of domains whose size is smaller than 1000 drastically decrease and domains with large size increase. In our simulation, the number of large size domains with the local fcc structure is more than that with the local hcp structure.

4. Summary and Discussion

In this paper, keeping crystallization of colloidal particles under a centrifugal force in mind, we carried out Brownian dynamics simulation and studied ordering of particles by a uniform external force. Especially, we focus the effect ordering of particles on walls on that in bulk and the dependence of ordering of particles on the external force.

When the external force is added to Brownian particles, the density of particles near the walls of a container increases, and ordering of particles on the walls starts. The layers of particles are formed parallel to the walls, which agrees with previous studies.[36–41] Then, ordering in bulk occurs in succession. As shown in Figs. 4 and 6, the particles attached on the wall act as substrate and epitaxial growth occurs. Thus, in order to form a large domain in bulk, it is necessary to make ordering of particles on wall well. In our simulation, ordering of particles on walls is better with a tilting force. Large domains of ordered particles are formed in bulk, which agrees with experiment.[13]

In our simulation, two walls cross orthogonally at an edge. If a $\{1, 1, 1\}$ face of the fcc structure or a $\{0, 0, 0, 1\}$ face of the hcp structure are formed on the two walls at a time, the expected faces of crystals formed in two walls cannot cross orthogonally. Thus, near the edge, where the distance of the two wall is very short, the formation of ordered structure is prevented and disordered particles appear. If we carry out the simulation with the system in which the two walls cross with a suitable angle $\alpha \neq 90^\circ$ at an edge, the nucleation can occur at the edge and ordering in bulk may become better.

Many defects are formed and both the fcc structure and the hcp structure are mixed in bulk in our simulation, which is probably because the Peclet number is so large and the volume fraction of particles is so high. In a previous study,[25] the fcc structure is formed with a low Peclet number and a low density of particles. Thus, if we carry out simulation with lower Peclet number and lower density of particles, the number of defects in bulk may decrease.

In our simulation, the ratio $n_{\mathrm{hcp}}/n_{\mathrm{fcc}}$ decreases with increasing the angle θ. Now, we do not have a simple idea to explain the result. In order to understand the mechanism, we intend to study the distribution of structures and the time evolution of the ratio in more detail.

Acknowledgments

This work is supported by Grants-in-Aid for Scientific Research from Japan Society for the Promotion of Science, and some parts of this study was carried out under the Joint Research Program of the Institute of Low Temperature Science, Hokkaido University.

References

1) T. Sawada, Y. Suzuki, A. Toyotama, and N. Iyi: Jpn. J. Appl. Phys. **40** (2001) L1226.
2) T. Kanai, T. Sawada, A. Toyotama, and K. Kitamura: Adv. Funct. Mater. **15** (2005) 25.
3) J. Yamanaka, M. Murai, Y. Iwayama, M. Yonese, K. Ito, and T. Sawada: J. Am. Chem. Soc. **126** (2004) 7156.
4) A. Toyotama, J. Yamanaka, M. Yonese, T. Sawada, and F. Uchida: J. Am. Chem. Soc. **129** (2007) 3044.
5) E. A. Kamenetzky, L. G. Magliocco, and H. P. Panzer: Science **263** (1994) 207.
6) J. M. Weissman, H. B. Sunkara, A. S. Tse, and S. A. Asher: Science **274** (1996) 956.
7) A. Blanco, E. Chomski, S. Grabtchak, M. Ibisate, S. John, S. W. Leonard, C. Lopez, F. Meseguer, H. Miguez, J. P. Mondia, G. A. Ozin, O. Toader, and H. M. Van Diel: Nature **405** (2000) 437.
8) Y. Yin, Z. Li, and Y. Xia: Langmuir **19** (2003) 622.
9) K. E. Davis, W. B. Russel, and W. J. Glantschnig: Science **245** (1983) 507.
10) A. Mori, S. Yanagiya, Y. Suzuki, T. Sawada, and K. Ito: J. Chem. Phys. **124** (2006) 174507.
11) A. Mori, Y. Suzuki, and S. Matsuno: Chem. Lett. **41** (2012) 1069.
12) Y. Suzuki, T. Sawada, and K. Tamura: J. Cryst. Growth **318** (2011) 780.
13) K. Hashimoto, A. Mori, K. Tamura, and Y. Suzuki: Jpn. J. Appl. Phys. **52** (2013) 030201.
14) M. Sato, H. Katsuno, and Y. Suzuki: Phys. Rev. E **87** (2013) 032403.
15) J. D. Weeks, D. Chandler, and H. C. Anderson: J. Chem. Phys. **54** (1971) 5237.
16) D. L. Ermak: J. Chem. Phys. **62** (1975) 4189.
17) H. Tanaka and T. Araki: Phys. Rev. Lett. **85** (2000) 1338.
18) Y. Nakayama and R. Yamamoto: Phys. Rev. E **71** (2005) 036707.
19) Y. Nakayama, K. Kim, and R. Yamamoto: Eur. Phys. J. E **26** (2008) 361.
20) Y. Matsuoka, T. Fukasawa, K. Higashitani, and R. Yamamoto: Phys. Rev. E **86** (2012) 051403.
21) Y. Nishijima, K. Ueno, S. Juodkazis, V. Mizeikis, H. Misawa, T. Tanimura, and K. Maeda: Opt. Express **15** (2007) 12979.

22) H. Mèguez, F. Meseguer, C. López, A. Misfud, J. S. Moya, and L. Vázquez: Langmuir **13** (1997) 6009.

23) P. Hoogenboom, D. Derks, P. Vergeer and A. van Blaaderen: J. Chem. Phys. 117 (2002) 11320.

24) J. Hilhorset, J. R. Wolters, and A. V. Petukhov: Cryst. Eng. comm 12 (2010) 3820.

25) M. Marechal, M. Hermes, and M. Dijkstra: J. Chem. Phys. 135 (2011) 034510.

26) R. Yamamoto and a. Onuki: J. Phys. Soc. Jpn. **66** (1997) 2545.

27) R. Yamamoto and a. Onuki: Phys. Rev. E **58** (1998) 3515.

28) T. Hamanaka and A. Onuki: Phys. Rev. E **74** (2006) 011506.

29) P. J. Steinhardt, D. R. Nelson, and M Ronchetti: Phys. Rev. B **28** (1983) 784.

30) M. D. Rintoul, and S. Torquato: J. Chem. Phys. **105** (1996) 9258.

31) W. Lechner and C. Dellago: J. Chem. Phys. **129** (2008) 114707.

32) L. Landau and E. Lifschitz, *Quantum Mechanics* (Pergamon, London, 1965).

33) A. Panaitescu, K. A. Reddy, and A. Kudrolli: Phys. Rev. Lett. **108** 108001 (2012).

34) C. Desgranges and J. Delhommelle: Phys. Rev. B **77** (2008) 054201.

35) B. I. Halperin and D. R. Nelson: Phys. Rev. Lett. **41** (1978) 121.

36) T. Fehr and H. Löwen: Phys. Rev. E **52** (1995) 4016.

37) Z. T. Németh and H. Löwen: Phys. Rev. E **59** (1999) 6824.

38) A. J. Archer, P. Hopkins, and M. Schmidt: Phys. Rev. E **75** (2007) 040501(R).

39) C. R. Nugent, K. V. Edmond, H. N. Patel, and E. R. Weeks: Phys. Rev. Lett. **99** (2007) 025702.

40) P. Scheidler, W. Kob, and K. Binder: J. Phys. Chem. B **108** (2004) 6673.

41) K. Watanabe, T. Kawasaki, and H. Tanaka: Nature materials **10** (2011) 512.